

HYPERVELOCITY IMPACT (HVI) SIGNAL ANALYSIS**Iiescu, L. E., Lakis, A. A. & Oulmane, A.**Mechanical Engineering Department, École Polytechnique of Montréal, Canada
C.P. 6079, Succursale Centre-ville, Montréal, Québec, Canada H3C 3A7**ABSTRACT**

Hypervelocity is a specific characteristic of the movement of space debris and micrometeoroids. Their high speeds in the space environment leads to major impact effects on a spacecraft surface or protection shield. Depending on the particle speed and diameter, the damage that occurs could lead to perforation of the spacecraft shell; a catastrophic failure of the spacecraft. The impact of these particles is a complex phenomenon that includes secondary ejecta, plasma or phase transformation of material. This paper presents the analysis of signals obtained from four hypervelocity impact tests, analysis done using specific software developed in-house by our research group as a bridge between theoretical research and practical applications of various vibration methods in different areas. This professional tool allowed us to calculate different time-frequency or time-scale transforms from the data file time signal. The application of two methods usually used for analyzing this type of signal, Choi-Williams distribution or Wavelet transform, allowed us to distinguish the characteristics of the two fundamental states of impacted targets; perforation and non-perforation. Based on these results, corroborated with further analysis and experimental tests, a dictionary of materials used for spacecraft protection will be created that includes automatic identification of space debris damage.

INTRODUCTION

Micrometeoroids and orbital debris (MMOD) represent the two main categories of space particles that travel at average velocities of 16 km/s and 9 km/s, respectively. Micrometeoroids are common space particles of small dimensions made of rock or metal that travel at velocities up to 20 km/s and pose a high risk for objects that spend long periods of time in space such as satellites. Orbital debris on the other hand, represents non-functional man-made objects that have been populating space since the first space launch in 1957. Since then, the number of such objects has grown to over 22 000 pieces. Space debris has different sources such as; satellite and rocket break-ups, satellite anomalies and mission related debris.

Impact between space vehicles and MMOD or impact between two such space-objects at the high velocities involved is called a hypervelocity impact (HVI). The intensity of these collisions produces a debris cloud and secondary ejecta with the potential to cause further damage, creating even more space debris. Two examples of such space events are the test on the defunct Fengyun-1C satellite in 2007, and the accidental collision of Iridium-33/Cosmos-2251 satellites in 2009. These events created approximately 5000 pieces of debris, most of them still in orbit.

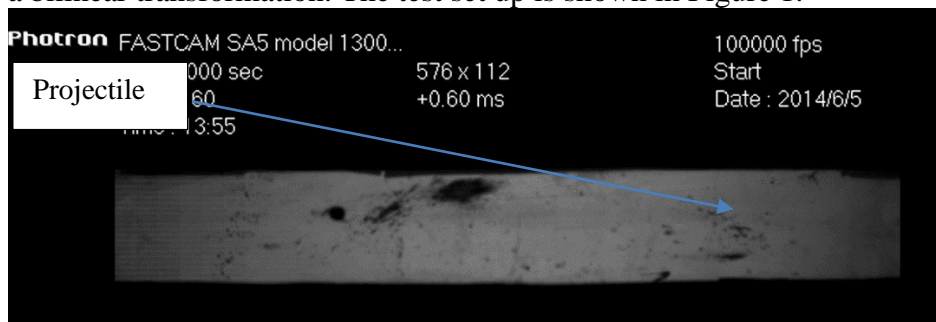
Existing ground systems cannot detect or track MMOD at sizes between 1 and 5 cm (diameter). These particle sizes pose the greatest threat to space vehicles. The development of new HVI protection devices that use new lighter materials could be a solution for mitigation of the impact effects of MMOD in this size range. HVI test data, which at this date is limited, would be very useful to aid research work in this area. Due to the extensive use of composite materials in spacecraft structures, characterization of HVI damage is complex. The phenomenon is controlled by failure thresholds and subsequent impact energy consumption [1, 2]. Improved

experimental and technical analysis development is essential to more fully evaluate the damage resulting from HVI impact.

This paper presents a method based on time-frequency analysis completed using in-house software. The approach provides advanced knowledge from HVI impact tests and damage analysis on different materials. Four test cases were analyzed with respect to spacecraft protection against orbital debris and micro-meteoroids [3]. The tests were performed at the Shock Wave Physics laboratory. The objective of the tests/analysis was to determine the essential characteristics of damage for two different materials; a metal (aluminium) and a carbon fiber (CFRP). Two different types of target status were analyzed; perforation and non-perforation.

This paper will represent a basis for further time frequency analysis of the signals in order to develop a method for automatic detection of HVI damage for different types of materials. In detail, the paper provides a time frequency analysis of the signals obtained from two sensors, one placed on the target (the main sensor used for the impact analysis) and the other outside of the testing chamber (an auxiliary sensor for impact confirmation and further analysis).

The two methods used are Wavelet Transform (WT) and Choi-Williams Distribution (CWD); a bilinear transformation. The test set up is shown in Figure 1.



a)



b)



c)

Figure 1: HVI testing video recording using FASTCAM a) target and sensor fixed in the testing chamber b) and c) testing chamber

This document is the second part [18] of a larger work that will potentially include (depending on availability of the test facility) further analysis of HVI tests at higher speeds (up to 8 km/s), the use of fiber glass (FBG) sensing technology to enable more accurate detection of HVI damage in real time and the automation of HVI damage detection.

THEORETICAL CONSIDERATIONS

General considerations

Impact theory and behavior is very well described by W. Goldsmith [19], who presents theoretical vibration aspects and dynamic processes as well as experimental results. The volume presents the impact as a function of the application, static or rapid loading, where the impacted material has a fluid behavior. Classical impact theory is a starting point; however it is not capable of describing the transient forces or deformations that occur in the case of impact. Our approach considers the vibration aspects of impact, examining the wave phenomena in order to specify the transient deformation and stresses.

Chapter V of the book is of particular interest since it includes a discussion of dynamic processes that lead to permanent deformations. Two approaches are described that could take these large strains and permanent deformations into consideration: the theory of hydrodynamic behavior of solids and the theory of plastic flow. The hydrodynamic theory of wave propagation in solids, which is usually employed in the study of HVI considers the target materials as a compressible fluid without shear resistance to derive the equation of state of different materials.

One element of impact vibration is related to the natural vibration of each of the two parts that are in contact following the transfer of impact energy. In our case the parts involved in the impact are the projectile and the target, and for this case projectile vibrations are neglected. For the particular case of an impact of a spherical projectile on a target, the contact force is described as a pressure distribution on the surface with variable amplitude. Hertz's contact law [23] refers to the localized stresses that occur when two curved surfaces come in contact and, due to the applied loads, deform slightly depending on the modulus of elasticity of the materials. This distribution is usually represented by an elliptical contact surface. Furthermore the impact force together with modal displacements of the target plate give rise to a forced transitory response materialized in a free vibration.

W. H. Prosser [20] analyzed the signals created by impacts on aluminium and graphite/epoxy composite targets in two different impact velocity regimes as both velocity and impact angle were varied. The signal in the low-velocity regime is dominated by a large flexural mode, with the overall amplitude increasing with velocity, mostly for the high-frequency components. Compared with the signal in HVI, both extensional and flexural mode components had comparable amplitude for non-penetrating impacts, but only an extensional component was evident when the target was perforated.

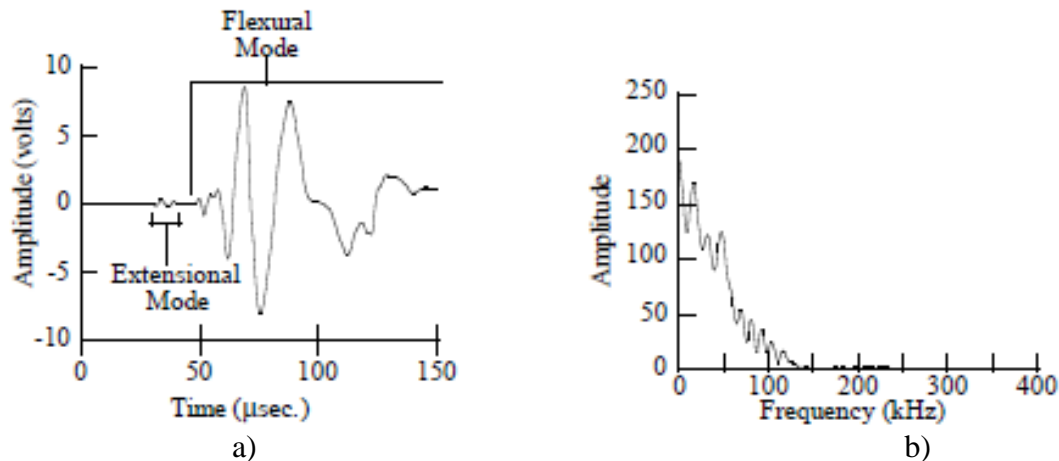


Figure 2: Low velocity impact on aluminium plates: a) The signal, b) The FFT of (a) [20]

Figure 2 presents the signals produced by a low-velocity impact. Extensional and flexural components can be noted, the extensional mode propagating with faster velocity and little dispersion compared with the flexural mode that travels at lower velocity and higher dispersion. The flexural mode is created by the off-mid plane source through the large bending that occurs because the projectiles at low-velocity did not perforate the target and instead created a larger target.

In his previous work, Prosser [21] studied the signals induced in a thin-walled graphite/epoxy tube (similar to the material at lay-up used by NASA for the struts of the space station) using lead breaks. Measurements of the velocities of the extensional and flexural modes were found to be in agreement with classical plate theory.

Our work, which is described in detail in paragraph 3 below, uses a comprehensive time frequency analysis tool – TF-Analysis developed by Prof. A. A. Lakis and his research team [22] in order to better characterize the HVI phenomena. More precisely, analysis of the impact signals obtained after a series of HVI tests led to identification of characteristics that allow us to differentiate the two essential types of target damage or conditions that occur in cases of non-perforation and perforation impacts, the latter of these being critical in the case of a spacecraft impacted by orbital debris or micro-meteoroids. Time frequency analysis was performed on two different materials, aluminium and composite. In further testing campaigns we will consider different types of materials used for spacecraft structure and MMOD protection in order to initiate development of a wide-ranging database of these materials; a dictionary of materials as a function of signal characteristics. Furthermore, the materials dictionary will be used for development of a fully automatic health monitoring system, capable of identifying in real time the type of damage that occurs in the case of HVI.

LITERATURE REVIEW

As following we have some similar work that was made in the area, the work mainly analyse different type of impact or damage based on Shock Response Spectrum (SRS) of the HVI vibrations. The J. B Vergniaud [23] paper investigates the modal response induced by the micrometeorits impact on a Gaia spacecraft and the disturbance created to the normal function of spacecraft sensitive instruments. More precise, the objective of the study is to assess the influence of the HVI on the dynamic response of the spacecraft and considers that previous

studies that considered spacecraft as nonflexible structure in order to predict stability in case of an impact momentum transfer are not sufficient.

In order to superimpose the dynamical impact response on a rigid spacecraft movement a realistic measurement of shock impact was necessary. Based on the Gaia mission coordinates, the paper classifies the impacts based on impact level (low, intermediate and high) and frequency of impacts (frequent to rare) and identify the typical micrometeoroid mass and velocity. For the HVI tests conditions they 2-stage light gun with the targets installed in the vacuum chamber hold in place with a very low frequency boundary conditions. The projectiles are launched at 3.5 to 7 km/s velocities at aluminium and CFRP sandwich panels. The analysis of tests results showed that the local stiffness of the target has the most important effect, the multiplication of skin thickness by two generates first modal response ten times higher, the reduced influence of honeycomb thickness and the second order of importance of the projectile parameters. Simulation and parameters descriptions were also done in order to correlate as well as possible with the tests results and to obtain an impact excitation function similar with the HVI. The study concluded that the regular micrometeoroids HVI will have a reduce influence on the Gaia instruments measurements.

Our study concentrates more on the damages that occur in the case of HVI that can significantly decrease the life expectation of an unmanned spacecraft, but the obtained results could be extended to analyse the influence to the accuracy of spacecraft equipment. Francesconi [24] presents a series of HVI test results in order to identify the main feature of impact induced vibrations on Al honeycomb sandwich panels and the influence to the spacecraft payload.

Furthermore the vibrations obtained were described through the shock response spectrum (SRS) of the three different types of waves that could be distinguished based on the acceleration directions. A series of thirty- four HVI tests were performed at velocities up to 5.8 km/s with Al projectiles of different diameters, and six acceleration signals were recorded for each test. The tests results were represented through the SRS of the recorded signals, distinction between the wave properties were noted in the case of penetration when the SRS could be one order on magnitude higher than the non-penetrating SRS. The study also evidenced the influence of projectile mass and impact velocity. In the next step a single empirical relation was derived using standard non-linear fitting methods in order to predict the shock response spectrum in the honeycomb sandwich panels used. The paper concluded that the HVI produces on the both side of the target a transient disturbance field that can be described through shock response spectra of out-plane, in-plane longitudinal and in-plane transversal waves.

Frank Schafer [25] study describes an impact sensor network and a mathematical model to determine the location of HVI. At first the paper discusses the advantages of such network, the position of sensor nodes and the basic requirements of such network. An efficient sensor system network should answer requirements as: time, position and strength of impact, and to offer a precise continuous real-time detection. The paper also introduce the wave propagation theory for the two types of target investigated and perform a throughout analysis of the ultrasonic signals. For the thin Al targets the longitudinal waves and for the honeycomb sandwich panels shear and bending waves beside the longitudinal waves in the facesheets. Localisation of the impact was made using an algorithm based on Pythagoras theorem used in combination with least squares method of minimization of the errors. The method revealed the correlation between the strong damping of the signal amplitude and increased localization uncertainty the Al- H/C SP compared with the Al plates and that the impact location could be predicted with almost the same accuracy indifferent of the waveform type. The system using ultrasonic

transducers was successfully tested on a spacecraft structure, showing that the peak signal amplitude recorded on Al plates exceeds those on Al-H/C SP by about order of magnitude and a localization algorithm was applied successfully using two different types of waveforms.

D. Pavarin [26] paper also analyses the propagation of shocks due to the HVI on the real spacecraft structure, the behavior of structural joints and based on the test results a database is created that links the impact conditions to the shock spectra. The paper is based on the extensive test results done at the CISAS HVI facility for the case of GOCE (Gravity Field and Steady-State Ocean Circulation Explorer) satellite as in Francesconi paper (). After a short description of GOCE mission and structural configuration HVI conditions were selected. The projectile diameters were chosen around 1 mm in order to induce a significant damage and based on the mission conditions. Four types of targets were also designed with different configuration using CFRP panels jointed together and mounted through an elastic suspension system (springs and dampers). The signal acquisition system used was using 30 accelerometers together with a laser velocimeter in order to have a comprehensive measurement and special data analysis software was developed. The results showed the extremely high-frequency content of the impact disturbances (several hundred kHz) with high acceleration levels (several hundred thousand m/s^2).

The specific of Gaia space mission was also made the object of G. Parzianello study [27] in order to establish a method that minimize the number of simulation needed to predict a Shock Response Spectrum experimental curve. The work analysed the effects of the input parameters on SRS and a method to combine and match an experimental signal using a Finite Element (FE) model. The frequency band used was 100—10000 Hz and the in order to study the effect of FEA parameters (mesh size, integration step or force impulse) two FEA software were used (Algor and Nastran). A particular attention was made to the experimental setup and the acquisition system in order to minimize the uncertainties of HVI tests on thin plates (3 mm). The presented method used a standard-shaped trapezoidal force impulse in order to show how SRS can be modified and scaled changing the force impulse properties based on comparing the simulations with the experimental result. The matching of the two curves could be done in a +/- 3dB band. Also the paper proposed a method to estimate the transport (a transport function) of the effect of standards impulses for different configurations.

Wavelet Transform

The wavelet transform (WT) is a time-frequency analysis method that gives good results in studying transient phenomena. WT associates time information to the frequency content, each wave being characterized by frequency band and arrival time. In literature there are few papers that present the application of WT to characterize the complex wave field that results in a case of HVI. One important remark is made by A. Bettela [11] in his paper that analyzes HVI waves with different amplitudes, content, velocities and direction of propagation that occur due to superimposition of vibration (original and reflected). More precisely, the paper tries to identify the fundamental constituents of this HVI disturbance field, the shock generation and transient vibration that can cause malfunctioning and breaking of sensitive electronic components on board a satellite.

The study of researcher Bettela present also an alternative method applied to the other analysis tools employed in the similar cases. For example, a Shock Response Spectrum (SRS) is used to evaluate the loads transferred in the case of HVI to the sensitive object through acceleration measurements without requiring characterizing the details of the source. The results are funded

by studying the morphology, speeds of propagation, frequency content, superposition, interference and reflection of waves.

The presented method starts from the mathematical form that describes the propagation of elastic waves in plates; the analytical equations are presented starting from 3D equations of waves for an elastic body with solutions which represent the constituent elements of real waves (3D harmonic wave). Full development of these calculations is presented in a book by Graff K.F. [12]. The solutions for the wave equations are represented by symmetrical (*S*) and anti-symmetrical (*A*), Lamb waves or guided waves, with different displacement modes. The WT method was validated through simulation and real HVI tests on Al plates using accelerometer measurements in order to identify by steps how the two wave modes (*S* and *A*) appear in WT spectrum.

The numerical signals showed that the *S* waves do not exhibit dispersive behavior, have unchanged shape and their frequency components travel at the same speed. The *A* waves present dispersive behavior (high frequency components have an earlier arrival time or travel faster and the low frequency ones in shorter time). Based on the results of experimental signal analysis for tests done on Al plates and honeycomb Al plates at low-speed and at hypervelocity, the paper concludes that two types of wave groups are observed, symmetric *SO* and anti-symmetric *AO* lamb waves. WT analysis is able to identify both the frequency content and propagation velocity. The experimental results were very effective for identifying the type of damage (with perforation or not) and concluded that, in the case of non-perforation, *AO* group waves are predominant and discontinuity (previous hole) is captured.

Lei Wang [13] investigates the existence of multiple higher-order Lamb wave modes in composites using piezoelectric sensors and ultrasonic frequencies. The paper studies the degradation and integrity of composite structures using ultrasonic transient waves for damage detection, localization and assessment of damage. In this case, due to the composite's multi-layer construction, heterogeneity of components and material anisotropy, the velocity of the wave depends on factors such as; laminate lay-up, direction of wave propagation, frequency and interface conditions. The paper identifies the different types of Lamb waves that occur due to impact on isotropic plates and multi-layer composites and presents two theoretical approaches used to investigate Lamb waves in composites: exact solutions using 3D elasticity theory (laborious computation of characteristic dispersion-transcendental equations) and approximate solutions using plate theories.

Continued development of our in-house software in the next steps of our work will create an opportunity for validation of our results by comparison with the results presented in the above-mentioned studies that relate the results of Lamb wave theory to impact damage identification.

Choi- Williams distribution function

The Choi–Williams distribution (CWD) function is part of the Cohen's class distribution function that uses an exponential kernel to suppress the cross-terms that result from the components that differ in both time and frequency.

H. Choi and W. J. Williams [14] introduce a time-frequency exponential distribution of L. Cohen's class and examine its properties. After interpretation of the distribution according to a spectral density–estimation point of view, they show how the exponential kernel controls the cross terms and analyze the result on two specific signals. They define the distribution for

discrete-time signals and, based on numerical example, conclude that the distribution is very effective in diminishing the effects of cross terms while retaining most of the properties of a time-frequency distribution.

CWD is mostly used in time frequency analysis of machinery vibration signals and machinery diagnostics. Howard A. Gaberson [15, 16] recognizes evidence of impact in examining the CWD performance on some machinery signals, which provide an impressive level of detail and a significant structure in the time frequency plane. Analyzing the accelerometer data taken from the intake valve cap on the head of the high-pressure cylinder of a large reciprocating compressor, he noted that the impact events showed a broadband, impact-like wide frequency content in the CWD contour plot and concluded that the CWD displays time frequency characteristics with the most precision.

In his paper, M. A. Hamstad [17] made a comparison between WT and CWD in order to determine the group velocities for different pairs of acoustic emissions (AE) sensors. Pairs of resonant or non-resonant wide-band AE sensors were used to sense the waves created by breaking pencil leads on an aluminum plate. The recorded signals were analyzed and processed by a WT. The group velocity curves (for the appropriate Lamb modes) were superimposed to clearly identify the modes in the signal. The arrival times at specific signal frequencies were determined (the time of the peak WT magnitude). The experimental group velocity was calculated based on the difference in arrival times and the difference in distance between the locations of the two sensors, and compared with the theoretical group velocity.

In his research, Hamstad used CWD as an alternate time frequency method following the same procedure and compared the experimental results with a finite element calculation. The main conclusions of the comparison between the use of WT or CWD to determine wave group velocities for the case of different AE recorded on relatively thin and large plates were:

- Determination of the arrival times of the two fundamental modes is relatively easy using either WT or CWD, independent of the type of sensor used (resonant or wideband)
- The experimental group velocities recorded were close to the theoretical values (less than 6.5 % difference)
- The high intensity regions determined using CWD occurred at a higher frequency compared with the frequency determined by WT (for each intense modal region). WT at higher frequency spreads the intensity from a single frequency.
- The CWD magnitude has sharper peaks as a function of time at lower signal frequency and as a function of frequency at higher signal frequency
- It can be expected that CWD provides more accurate arrival time results than WT for thicker plates (more modes closer in time).

TF-Analysis software

TF-Analysis software was developed at Polytechnique by Prof. Lakis A, A. and the research team [7]. It offers a wide range of methods in time, frequency, time-frequency analysis and wavelet transforms, see Figure 3. It also offers more advanced techniques in the recently-developed domain of automatic classification of rotating machinery using image processing by application of Fourier descriptors and neural networks [22].

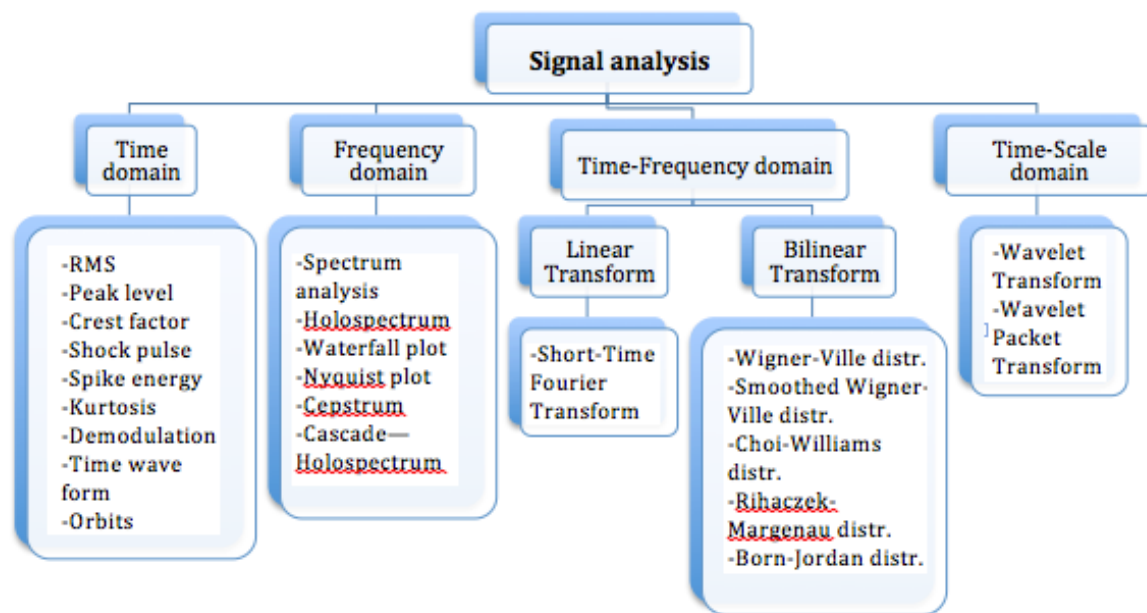


Figure 3: Features in TF-Analysis.

Work performed and attained objectives

In order to find distinguishable characteristics of HVI impact that will enable classification of different materials used in aerospace our group performed extensive work that covers the following main tasks:

- HVI testing campaign on two different target materials, covering both considered conditions of target, performed using a low-velocity launcher
- Analysis of signals from sensors mounted on the testing chamber in order to assess the identification of impacts from a signal captured outside the target, the case of perforation of an outside bumper of an MMOD protection system, and a signal captured on the spacecraft shell.
- Assess target damage and analysis of this signal using different time frequency analysis methods and identifying the methods with the best results
- Centralize the results in order to observe differences and similarities between analysis outcomes

The above steps are discussed in detail in the following sections of this paper.

HVI experimental testing

Six signals were recorded during the HVI testing campaign performed at Shock Wave Physics laboratory of Montreal. Projectiles were shot onto aluminum and carbon fiber targets using a gas launcher at different gas pressures (2000 Psi to 4000 Psi). Projectile velocities ranged from 560 to 1670 m/s.

The projectile launcher is driven by high pressure helium gas using a double diaphragm propulsion mechanism and a polycarbonate sabot. A rare earth magnet NdFeB, MAGCRAFT is used to determine the velocity of the projectile. As the stripping mechanism, an essential factor, a dynamic method that utilizes a heavier gas than He, Nitrogen (N₂), is used. The method has an unwanted effect; a secondary impact caused by the sabot.

A second separation mechanism could be used in future tests to deflect the sabot from its original trajectory so that it does not hit the sample and thus avoid inducing unwanted noise in the signal. The materials used as targets were:

- Aluminum 6061-T6; two thicknesses, approx. 1 and 5 mm

Material	Nominal density lbs./cu.in.	Tensile strength psi	Fatigue strength psi	Shear strength psi
Al 6061-T6	0.0975	45,000	14,000	30,000

- Carbon fiber/Epoxy rigid composite sheet of 3.175 mm thickness

Material	Nominal density lbs./cu.in.	Tensile strength psi	Compressive strength psi	Flexural strength psi
High-strength lightweight rigid carbon fiber	0.05-0.067	120,000-175,000	75,000-128,000	89,000-174,000

The material choice was made in order to create at least two types of hypervelocity impact damage, crater and perforation, in two different materials and also to consider other factors such as material review, market availability, test facility availability and the timeframe. More precise results of HVI could be achieved by applying a vacuum to the test chamber. This was not done for these experiments due to the timeframe of this project and the target design requirements. This option could be considered for future tests at the later stages. For the next tests it is probable that the targets will be suspended at four points and mounted using a vibration acquisition system. This set up should allow more precise signal analysis. The data acquisition system used for the preliminary signals was a Ni PXIe-1062Q [4] coupled with three accelerometers, one mounted on the sample and other two mounted on the outside of the testing section. LabView software was used to convert the analog signal to digital and store the signals on a PC.

To convert the impact vibration into a signal for the testing session, analog sensors, accelerometers with very high sensitivity ranging from 0.1 to 10.2 mv/ (m/s²), were used. For these testing sessions PCB Piezotronics model 352C33 accelerometers were considered suitable [4]. Two sensors were used to record valid impact signals. One was mounted on the target at a fixed position in order to not influence the signal. The distance from impact was variable due to the imprecision of the shots. The images show that the distance is around 30 mm (+/- 5 mm). The second sensor was mounted on the outside of the testing chamber, inside of which the targets were mounted.

During the test a frequency sampling rate of 50 KHz\0A was used. For signal analysis the WT was mainly a linear distribution at different levels of decomposition (level 5 is presented in images) with different time and frequency window lengths and using a Daubechies filter. In order to have a distinct difference in frequency amplitude we used various bi-linear transformations and we selected the Choi-Williams distribution results (a member of Cohen's class distribution that suppress the cross terms) to be presented in this paper.

The uncertainty analysis

The HVI tests setup is based on the installation of shock wave laboratory, with a particular attention that was made in selecting the acquisition system for measuring the impact

accelerations. A description of the test facility with details on the different sources of uncertainties related to test campaign performed could be found in the previous work [18]. D Pavarin [28] paper presents detailed discussions on the different sources of uncertainties related to the measurements of the vibrations in the case of HVI tests.

The precise measurement of the accelerations was assured by the particularities of the installation used that minimize the mechanical shock and vibration transmitted to the impact installation and by the fact that there is no ignition or combustion of the gun powder as in a 2-stage light gas guns. In the case of the mechanical sabot catcher we could have had also perturbations, another reason that this solution was not used. Other source of perturbations that we considered was the gas that is expelled in the vacuum chamber with the possible small fragments of the diaphragms and the second impact of the sabot. The measurement instrumentation and data acquisition system was based on the accelerometers used, that have a dynamic range and bandwidth selected based on the target type, the distance from the impact location and the specifics of the target assembly.

Introduction of test results analysis; preparatory work

Four tests were analyzed using the TF-Analysis in-house software [6-8], Table 1 summarizes the testing conditions and signal recording durations. Amplitude and shape were compared for each signal. Signals were recorded from the two sensors (on target and outside) in order to correctly identify the damage (penetration or non-penetration) on two types of material, aluminum and carbon fiber.

Table 1: Test summary

Test No.	Sample	Thickness (mm)	Projectile (sphere, mm)	Velocity (m/s)	Duration (Min:sec)	Damage characteristics
Test 1	CF	3.175	3.2	1570	2:12	Penetration
Test 2	CF	3.175	3.2	880	1:53	No Penetration
Test 3	Al6061 T6	0.8128	3.2	570	0:45	Penetration
Test 4	Al6061 T6	4.826	3.2	540	0:10	No Penetration

Due to computation limitations the larger signals (one, two and three) couldn't be analyzed over the entire duration. These had to be segmented into multiple signals, each with a maximum duration of 40 s, and analyzed separately to determine the moment of impact. Also, in order to analyze the signal in detail, and more importantly to be able to use all the software functions and cover all time frequency analysis methods, the signal was segmented into time-intervals of 40 ms.

Signal obtained from the sensor mounted on the outside of the test chamber

In addition to the on-target sensor, a secondary sensor mounted on the outside of the test chamber was used, see Figure 4. This sensor is necessary to have a precise recording of the impact.



Secondary sensor

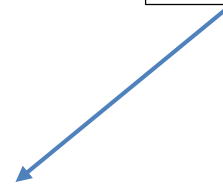
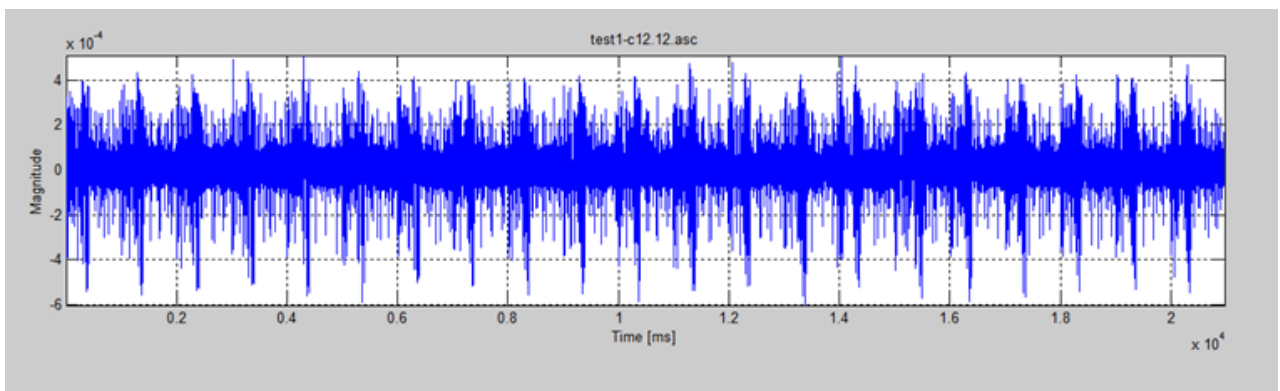
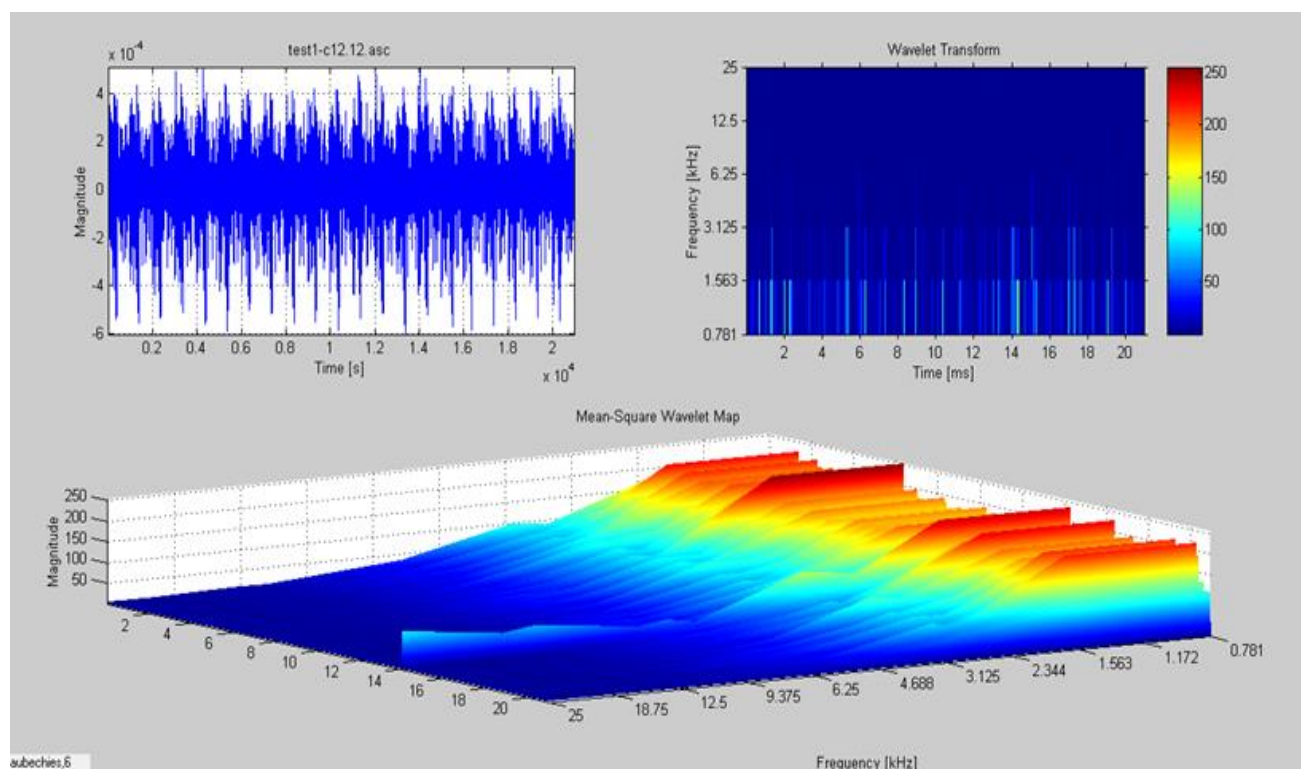


Figure 4: Position of the sensor mounted on the outside of the test chamber

The signal recorded from this sensor showed that the impact can be captured and distinctly identified in a signal recorded on a complex structure at a certain distance from the impacted target, such as on the last bumper or interior wall in the case of a complex orbital debris protection system (shield). One of the recordings of the sensor mounted outside the test chamber (corresponding to Test 1) is presented in the following image, Figure 5.



a)



b)

Figure 5: a) Signal recordings from Test 1, b) the time frequency representation of WT.

The outside sensor captured all four impacts for the four tests. The above image corresponds to Test 1 performed on CFRP and indicates perforation of the target. This fact is revealed only by the WT (Figure 5b). In the first graph, in time dimension (Figure 5a), the impact cannot be distinguished. Also, we notice that for the sensor mounted on the outside of the target the amplitude of all signals in time is of order 10^{-4} . The above analysis represents only a section of Test 1; 20 seconds corresponding to approximately 1 million recording points.

For the second test, Test 2 on CFRP with non-penetration, the moment of impact is again seen on the time frequency graph of the WT. The same variation in frequency amplitude occurs over the entire time domain. In this case the frequency variation is more attenuated than in Test 1. The WT signal analysis of Test 3 on aluminum (Al) with perforation as a result, also shows the impact on the time frequency graph with the same variation in frequency amplitude over the entire time domain, but with a slightly different form and with higher frequency amplitude due to a more rigid Al target.

As in previous tests, the Test 4 impact, on thicker Al plate with non-penetration as a result, was captured by the outside sensor. The time frequency graph of the WT showed the same variation in frequency amplitude over the entire time domain. This variation was more attenuated than in Tests 1 and 2 with the CFRP target. The shape of the graph was similar to that of Test 3 (on Al).

Due to the short length of the signal, 10 seconds (approximately 500000 points), it could be analyzed entirely and it was not required to use sections. In conclusion, impacts can be identified using a sensor mounted outside the impacting area on a continuous structure using the TF-Analysis software. Furthermore, this approach works for different materials and different types of damage.

MATERIAL DAMAGE AND SIGNAL ANALYSIS

Tests on a CFRP target, penetrated by a projectile

Figure 6 represents the target damage corresponding to Test 1, CFRP at 3,175 mm thickness with 1.57 km/s impact velocity. Visual inspection of the target reveals three types of damage:

- Primary damage: perforation, due to projectile impact
- Secondary damage: non perforation, from the impacting fragments (18-20 fragments of very small and varied dimensions), dispersed on a 6 cm diameter area
- Sabot damage: non-perforation, impact of lower intensity
-
-

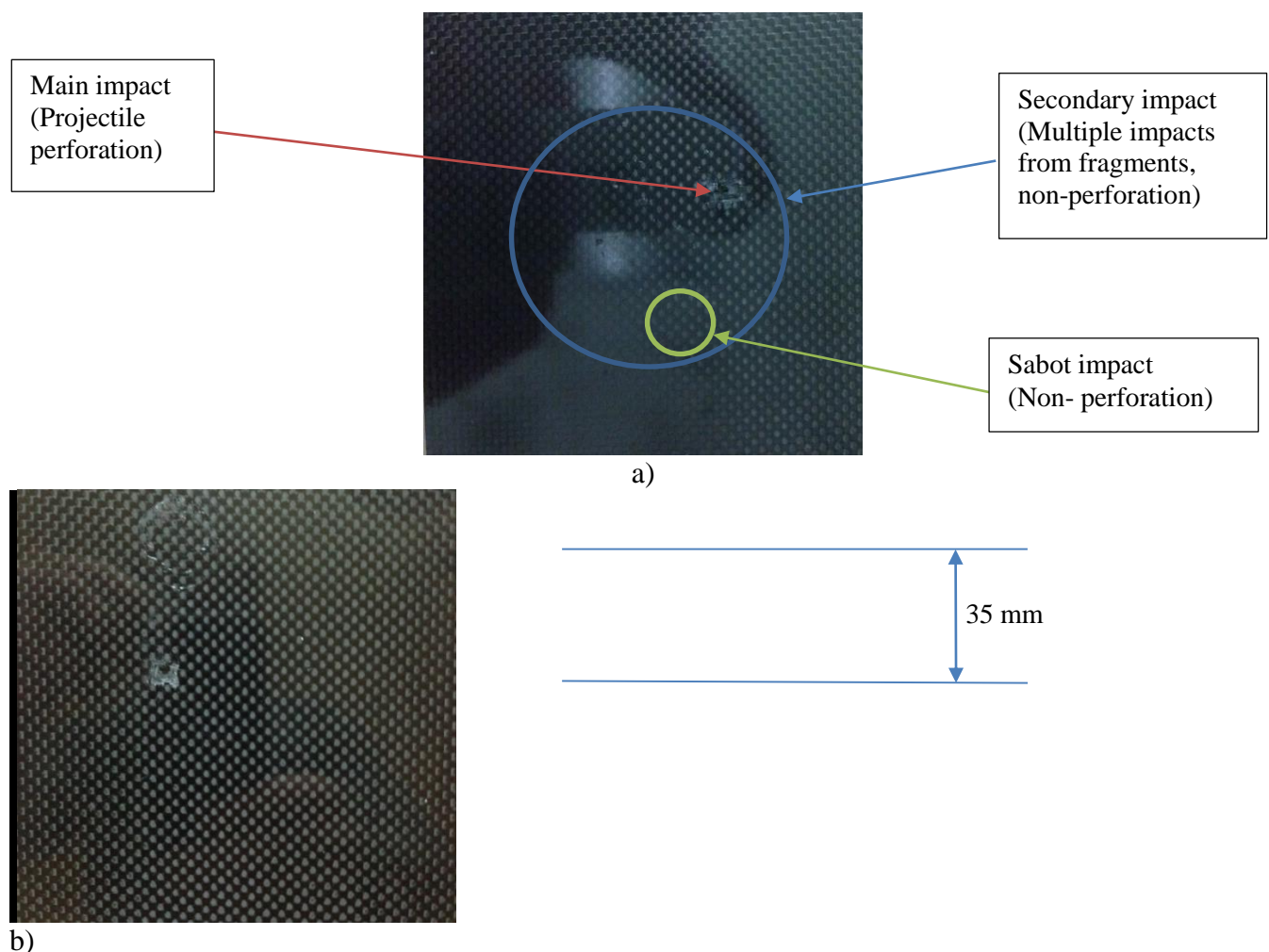
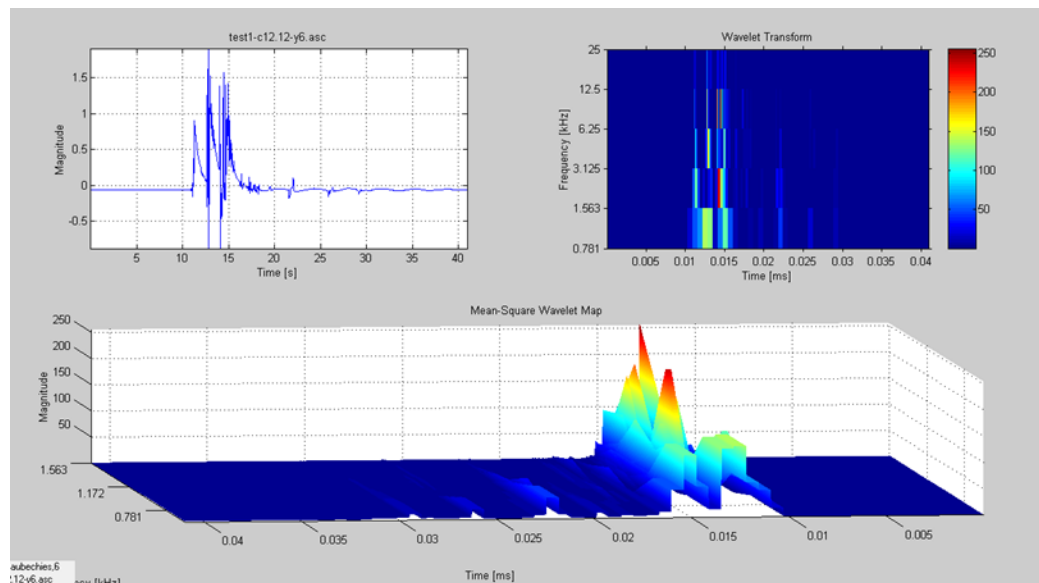
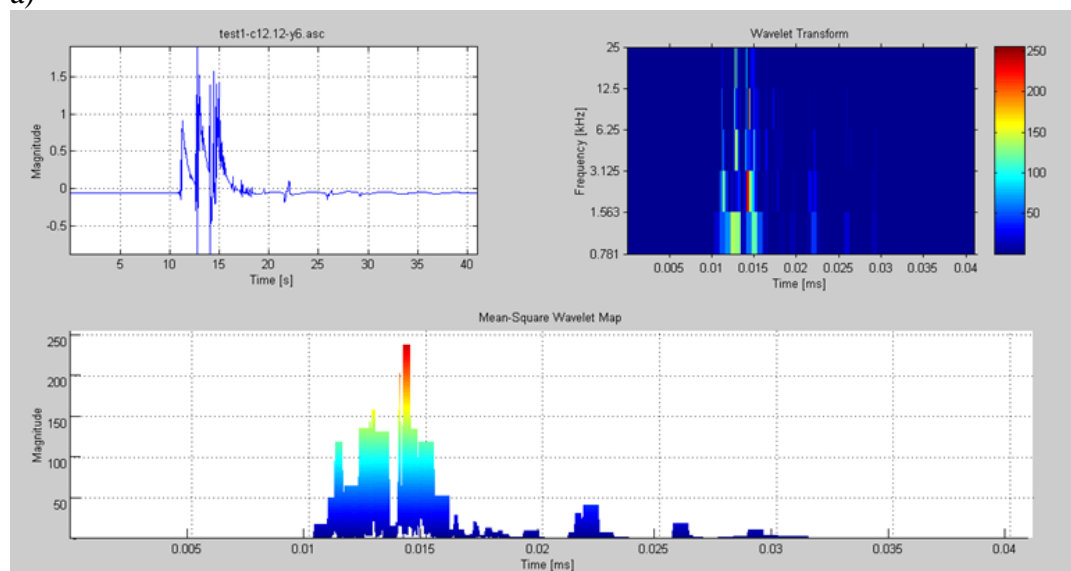


Figure 6: Impact damage on test1 CFRP 3.175 mm, fully perforated face a) and back b)

Figure 7 represents the recording and WT for the signal captured by the sensor mounted on the CFRP target



a)



b)

Figure 7: On-target mounted sensor, Test 1 signal recording and WT shape a) and profile b)

On the WT graph, three frequency peaks are noted that correspond to the three types of impact, perforation, secondary multiple impact, and sabot impact. The shape of the impact transform is the essential element that should be noted. The large amplitudes are compressed in a 5 ms interval and the width of the peaks at maximum amplitudes is only a few μ s. The Choi- Williams distribution for the Test 1 signal is presented in Figure 8

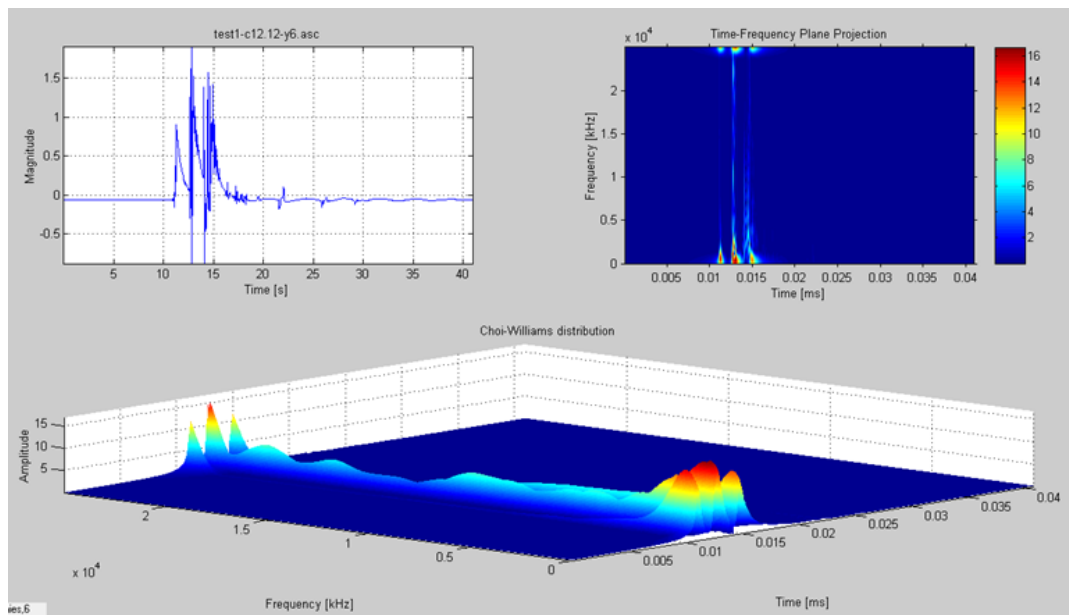


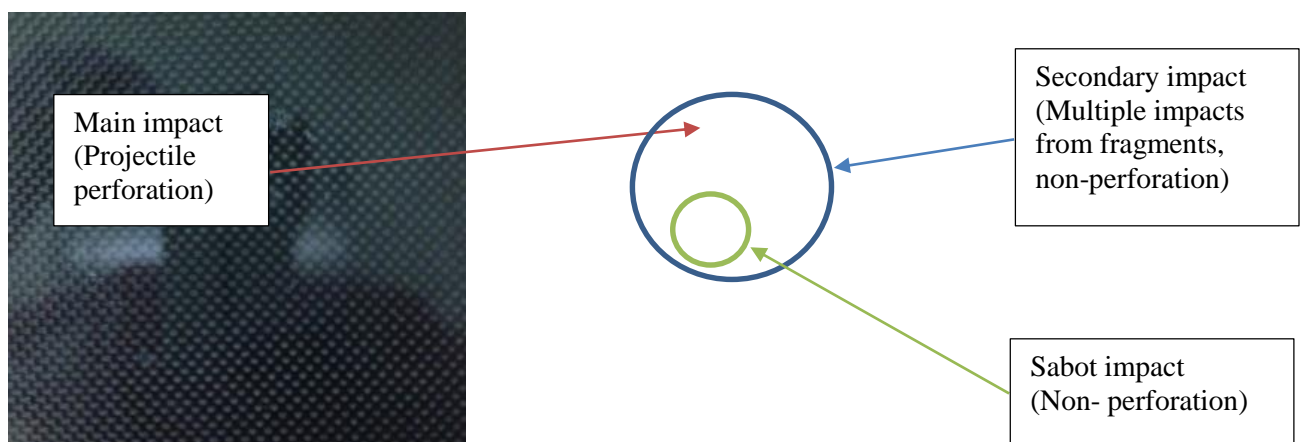
Figure 8: CWD corresponding to Test 1 signal

The time frequency analysis shows the corresponding three peaks, but the most important detail is the frequency amplitude, for a CFRP perforated target the maximum amplitude is 15.

Test on CFRP target, not penetrated by a projectile

Figure 9 presents the target damage corresponding to Test 2, on CFRP at the same thickness as Test 1 but impacted at lower velocity; 0.88 km/s. In this case the target is non-penetrated. Visual inspection of the target reveals three types of damage:

- Primary damage: non-perforation, due to the projectile impact
- Secondary damage: non-perforation, fewer impacts from fragments (3-5 fragments), over a 4.5 cm diameter area
- Sabot damage: non-perforation, impact of lower intensity
-



a)

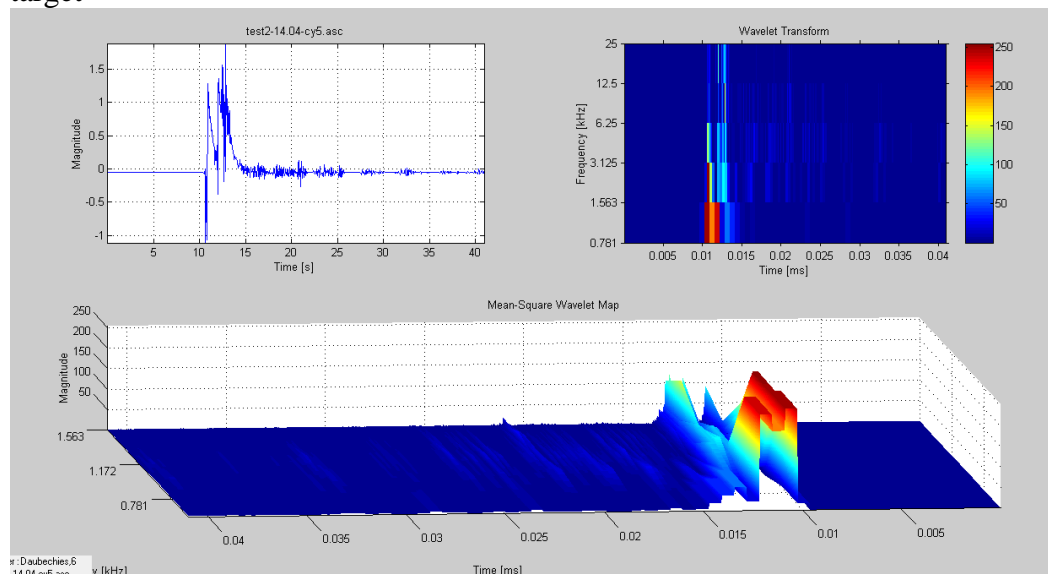


b)

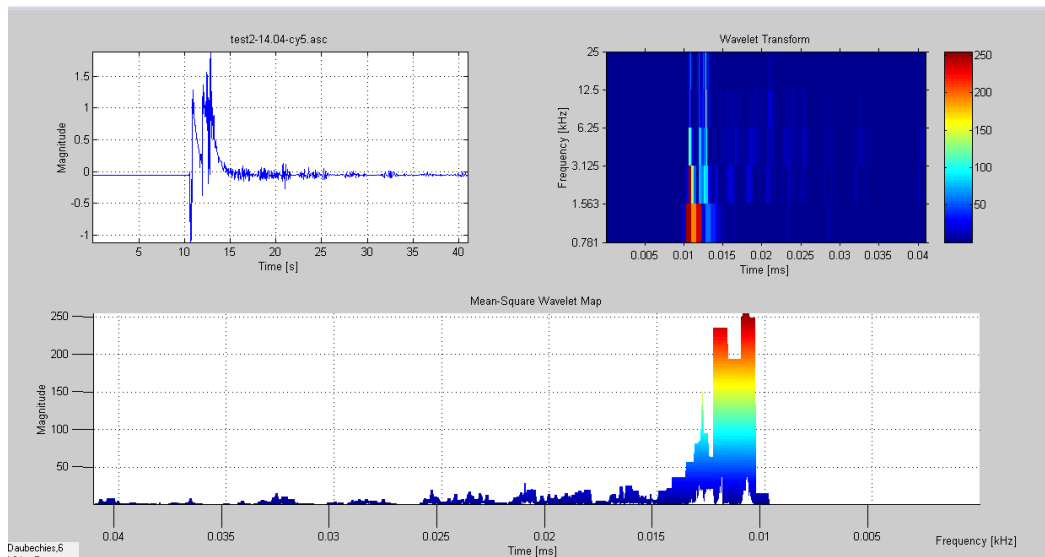
Figure 9: Impact damage for Test2, CFRP 3.175 mm, non-perforated face a) and back b)

The recordings and time frequency analysis that correspond to Test 2 are shown on the following Figures.

Figure 10 presents the recording and WT for the signal captured by the sensor mounted on the target



a)



b)
Figure 10: On-target sensor, Test 2 signal recording and WT shape a) and profile b)

The time frequency graph shows the same three frequency peaks that correspond to the three impacts, projectile, secondary multiple impacts and sabot impact. However this time only two peaks are more accentuated. The shape of the WT has changed, the signal is shorter in time (less than 5 ms), and at maximum amplitude the width of the peaks is more than 1 ms. As can be seen in *Figure 10a*, the first and second frequency peaks are compressed together at almost the same amplitude.

The Choi- Williams distribution for the Test 2 signal is presented in *Figure 11*.

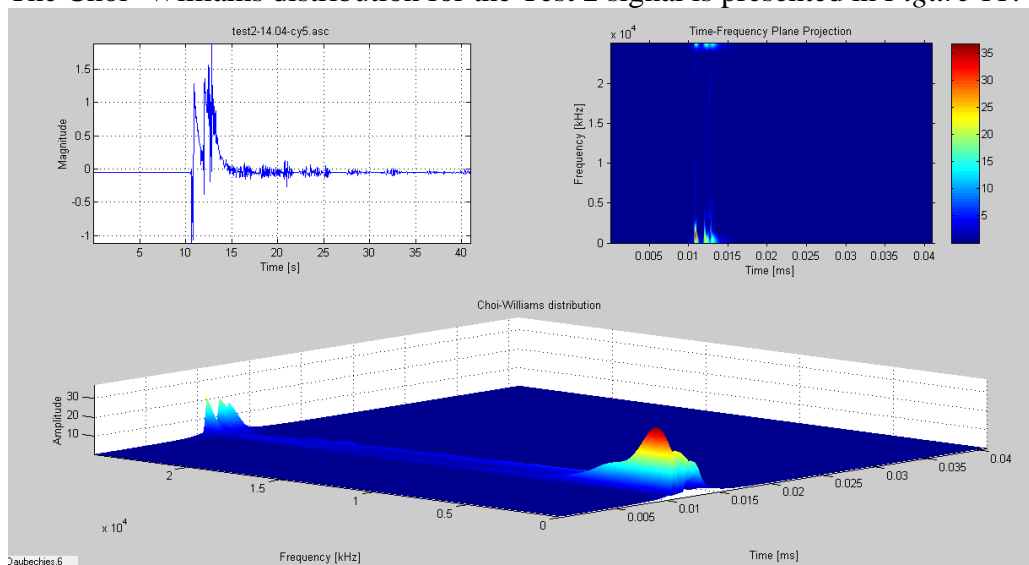


Figure 11: CWD corresponding to Test 2 signal

The time frequency graph shows the corresponding three peaks with one peak more pronounced, but the most important detail is the frequency amplitude which, for a CFRP non-perforated target, has a maximum around 30. This value, double that shown in Test 1, is an important indication of non-penetration. The material absorbed the vibration (large peaks, smaller propagation in time), amplifying the maximum frequency.

Test on an Al target, penetrated by a projectile

Figure 12 presents the target damage corresponding to Test 3, an Aluminum target approx. 1 mm thick impacted at a velocity of 0.57 km/s. The target is penetrated by the impact. Visual inspection of the target again reveals three types of damage:

- Primary damage: perforation due to projectile impact
- Secondary damage: non perforation, fewer impacts from fragments (3 fragments), over a 3.5 cm diameter area and one small perforation (less than 1 mm from one fragment)
- Sabot damage: non-perforation, impact of lower intensity

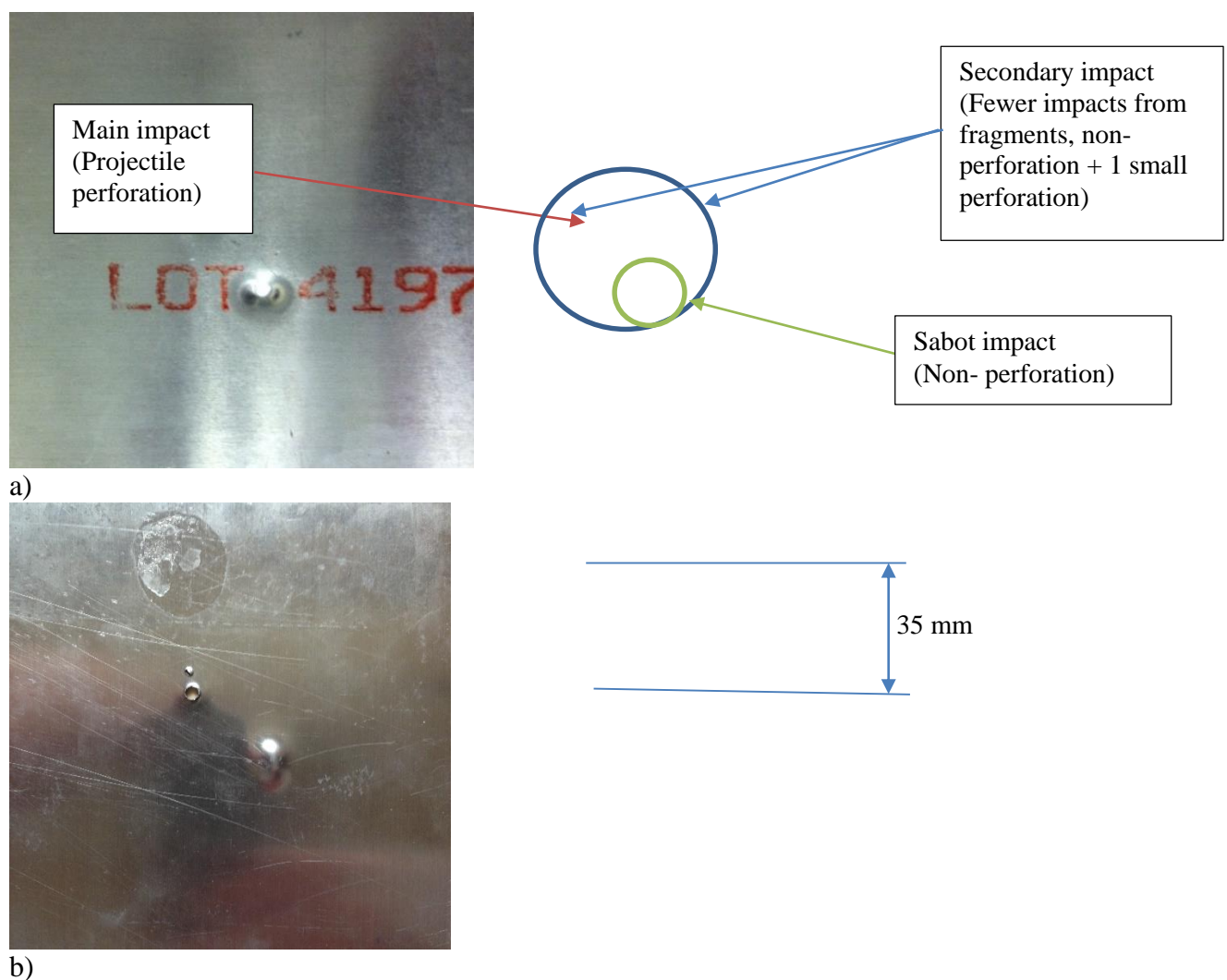
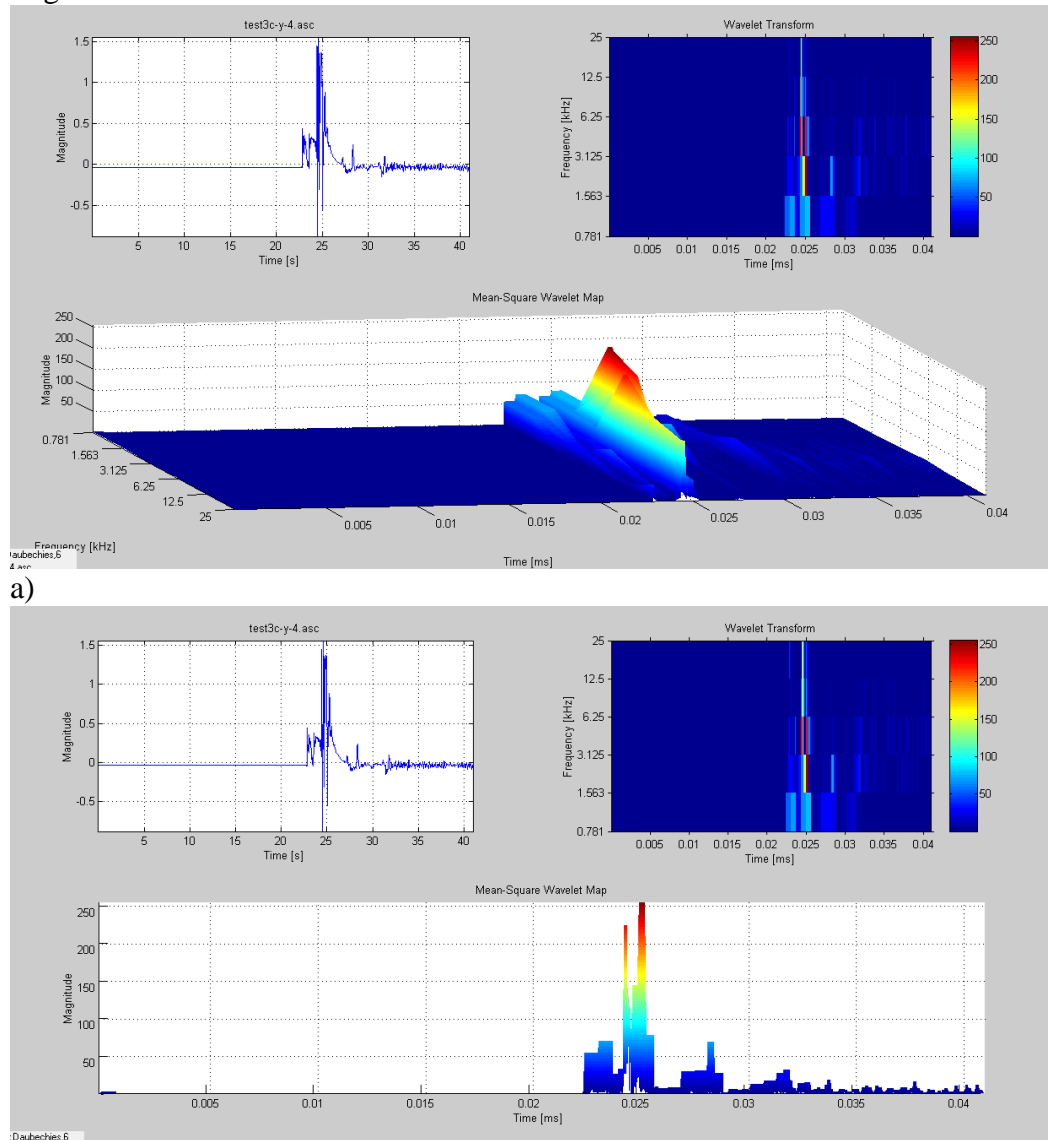


Figure 12: Impact damage on Test 3 Al, perforated face a) and back b)

The recordings and time frequency analysis that correspond to Test 3 are presented on the following Figures.

Figure 13 presents the recording and WT for the signal captured by the sensor mounted on the target



b) Figure 13: On-target sensor, Test 3 signal recording and WT shape a) and profile b)

The WT shows the same two frequency peaks corresponding to the projectile perforation and the fragment secondary non-perforation, along with multiple lower amplitude peaks corresponding to secondary multiple impacts and sabot impact. The form of the impact is cleaner, over an interval of 5 ms, and the width of the peaks at maximum amplitude is in the μ s range. Similar to Test 1, the WT has the same shape, which seems to be characteristic of penetration. As can be seen in Figure 13 b, the first and second frequency peaks are compressed together and at almost the same amplitude.

The Choi- Williams distribution for the Test 3 signal on aluminum is presented in Figure 14.

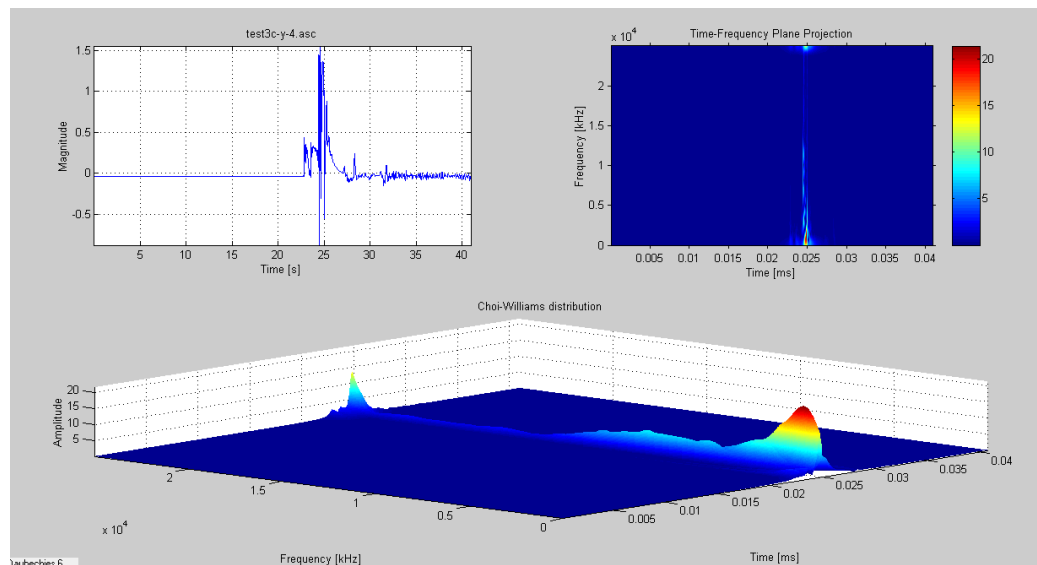


Figure 14: CWD corresponding to Test 3 signal

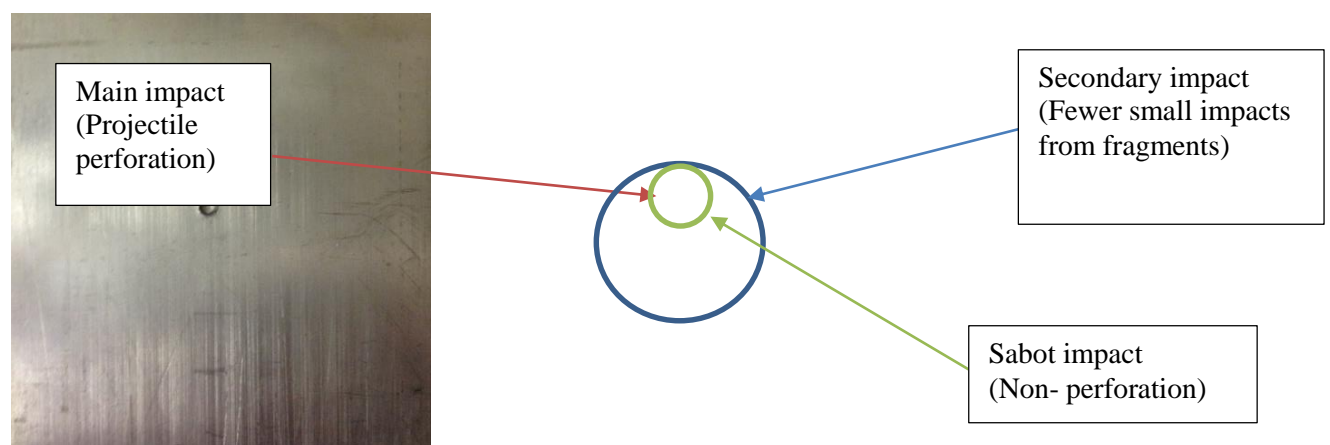
The CWD shows one much accentuated peak and a few non-significant very small amplitude peaks. Again observing the frequency amplitude, the maximum value for an Al perforated target is about 20 which is higher than the value recorded for Test 1 on a CFRP target (amplitude 15). The material characteristics narrowed on a shorter period of time with large accelerations and, due to the higher rigidity of Al, the CWD shows a higher maximum amplitude of frequency than the previous similar test.

HVI test on an Al target not-penetrated by a projectile

Figure 15 presents the target damage corresponding to Test 4, an Aluminum target at approx. 5 mm thickness impacted at a velocity of 0.54 km/s. No penetration damage occurred. For this case the velocity was kept approximately constant and the thickness of the Al was increased in order to achieve a non-perforation result.

Visual inspection of the target reveals the same three types of damage:

- Primary damage: non-perforation, from the projectile impact.
- Secondary damage: non perforation, fewer impacts from fragments (1-3 fragments), over a 3 cm diameter area.
- Sabot damage: non-perforation, impact of lower intensity
-



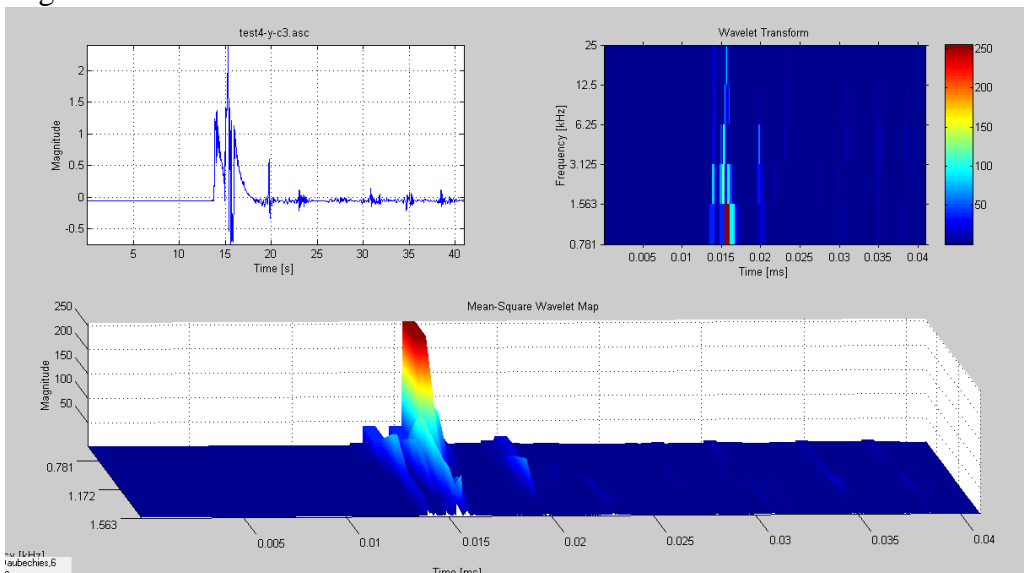
a)



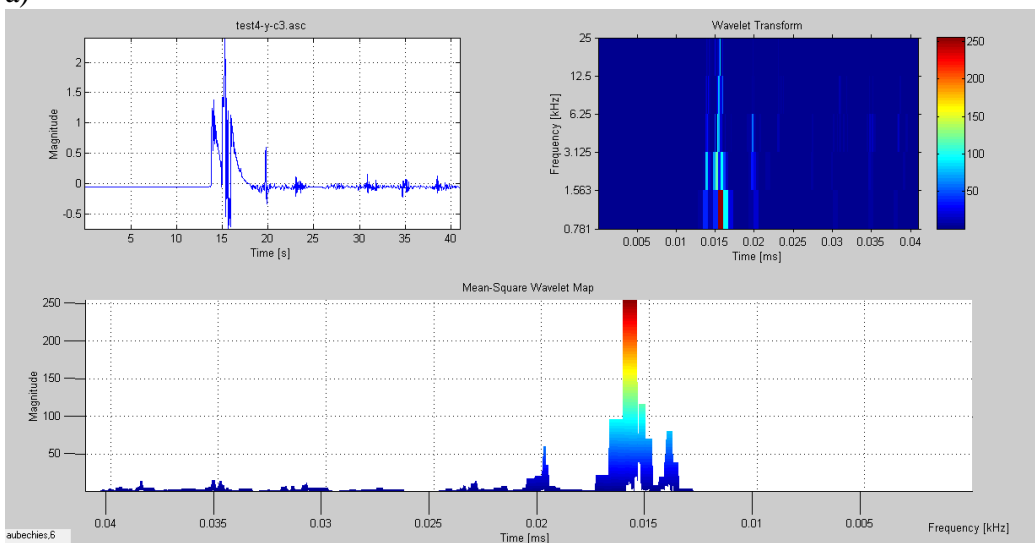
b)

Figure 15: Impact damage on Test 4 Al, non-perforated, face a) and back b)

The recordings and analysis that correspond to Test 4 are presented on the following Figures. Figure 16 presents the recording and WT for the signal captured by the sensor mounted on the target.



a)



b)

Figure 16: On-target sensor, Test 4 signal recording and WT shape a) and profile b)

The time frequency analysis shows one very well defined frequency peak that corresponds to the projectile impact and two lower peaks corresponding to secondary and sabot impacts. The form of the impact shows two characteristics: the cleanness of the signal (not a multitude of peaks) over a time interval of 2 ms, characteristic to the more rigid material (Al), and the width of the maximum amplitude frequency peak of more than 1 ms. The width of the peak is similar to that of the non- penetrating Test 2 on CFRP. The recorded signal has a compressed form, shown in Figure 16a.

The Choi- Williams distribution for the Test 4 signal is presented in Figure 17.

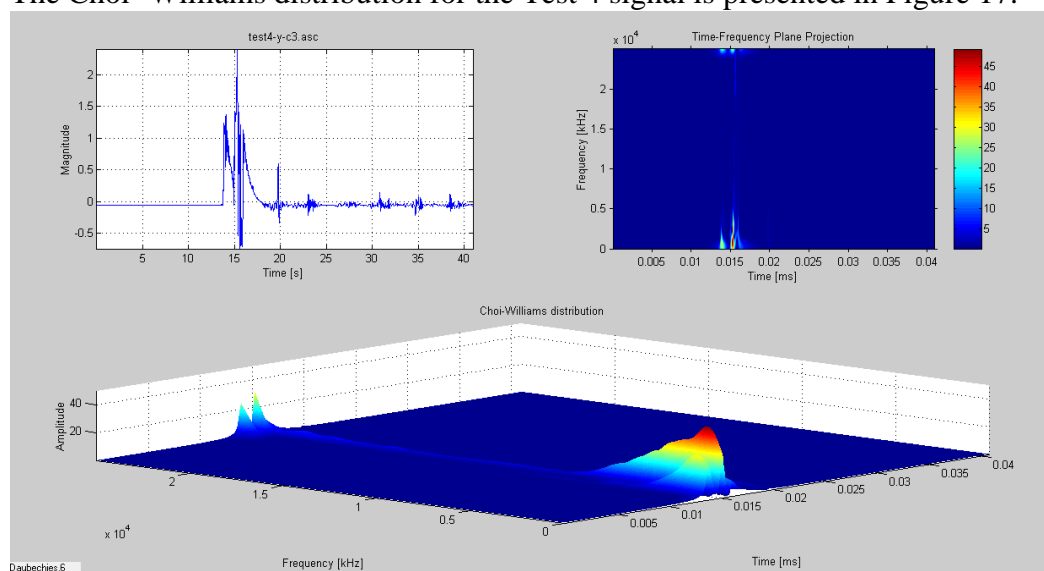


Figure 17: CWT corresponding to Test 4 signal

The CWD shows only the two peaks corresponding to the projectile impact and the fragment impact. The factor that really represents the damage is the frequency amplitude. In this case of an Al non- perforated target, the maximum value is about 40. This value is double that of Test 3 and could represent an important indication of non-penetration. The material absorbed the vibration (large peaks, smaller propagation in time), amplifying the maximum frequency.

SUMMARY OF THE ANALYSIS AND DISCUSSION

A comparative summary of the analysis completed for the four tests is presented in Table 2.

Table 2: Summary of the analysis

Test No.	Material, thickness (mm)	Damage characteristics*	Shape of the signal	Width of signal peaks	Frequency amplitude	Max. frequency range (kHz)	Impact detected by non-target sensor
Test 1	CF, 3.175	Penetration See Figure 4	Multiple peaks compacted in more than 5 ms	Thin profile of few μ s width	15	1.563 to 3.125	yes
Test 2	CF 3.175	No Penetration See Figure 7	Less peaks compacted	Large profile of	30	0.781 to 1.563	yes

Test No.	Material, thickness (mm)	Damage characteristics*	Shape of the signal	Width of signal peaks	Frequency amplitude	Max. frequency range (kHz)	Impact detected by non-target sensor
			in a smaller time interval less than 5 ms	peaks of more than 1 ms width			
Test 3	Al, 0.8128	Penetration See <i>Figure 10</i>	Clean shape with fewer peaks on an approx. 5ms time interval	Thin profile of few μ s width	20	1.563 to 3.125	yes
Test 4	Al, 4.826	No Penetration See <i>Figure 13</i>	Cleaner shape with two peaks on an approx. 2-3ms time interval	Large profile of peaks of more than 1 ms width	40	0.781 to 1.563	yes

- * 1) No stress or tension measurements were performed on the samples after the tests
 2) The test results are only visually analyzed
 3) The results represent a basis for a future study on different materials used in aerospace for protection against orbital debris impacts. This future study will allow creation of a functional dictionary of these materials

Table 2 clearly shows the differences between the signal characteristics for the cases of penetration and non-penetration impact: shape, peak profile and maximum frequency range. Using the same characteristics we can also differentiate the materials; the more rigid material presents shapes that are cleaner, shorter and with less reverberation in time. The most important factor that can be used to identify the damage type (penetration or non-penetration) for different types of materials (Al or CFRP) is the frequency amplitude. The amplitude doubles for the case of non-penetration for both materials and is five points lower for the less rigid material.

It is important to discuss the particularities of our experiments and analysis. The results are based on a small number of tests and should be validated by future tests or virtual simulations. The conditions of the HVI tests changed slightly from one test to another. Although we tried to keep the same projectile velocity, it was not possible because we had to simulate different types of damage. Also, the characteristics of the launcher combined with the timeframe didn't allow better control of the velocity. It is preferred to eliminate secondary impacts from fragments and the sabot to generate a cleaner signal. To achieve this, use of a mechanical stripper is envisaged for future tests. Other factors that could improve the data and the quality of our analysis in future tests include: more precise shots with a constant distance between the location of impact and the location of the sensor, and use of a second recording device to capture signals at the moment of impact.

Even without these improvements, the results of our four tests show clear trends for different types of damage and different types of materials. Nevertheless the execution of future tests and simulations on an extended aerospace material database is a must in order to have the necessary

premises for the creation of an automatic material dictionary and real-time monitoring of the health of the protection system.

CONCLUSIONS

Analysis of signals recorded during HVI tests performed at the Shock Wave Laboratory provided valid outcomes that can be used as a starting point in the development of a tool capable of real-time detection and analysis of the effects of MMOD impacts. A review of related theory offers a basis for understanding how different materials will show different behavior in case of hypervelocity impact. Our specific test series aimed at exploring the differences between CFRP and Al from the point of view of recorded signal analysis. For Aluminium, the more rigid of the two materials, the amplitudes of the recorded signals were higher than those recorded for CFRP.

Time frequency analysis was carried out for the signals recorded by both (2) sensors; one mounted on the target and the other mounted on the exterior of the test chamber outside the testing area (the chamber was not placed under vacuum for these tests). During the test sessions, different recording durations were used to see how the impact signal distinguished itself over time. This increased the total duration of the time frequency analysis, and each signal had to be sectioned into time intervals to allow use of our software at full capacity and also to work within the available computation capacity. For example, the number of points for Test 1 (performed on CFRP) was reduced from 7 million points to 3000 points and even lower to 100 points, representing a time decrease from over 2 minutes to microseconds. This reduction allowed deeper analysis of the recorded impact. For our purposes a time frequency analysis in the millisecond range was sufficient because it allowed us to use all other linear and bilinear transformations besides WT, such as the presented Choi- Williams distribution which provided clear information related to the amplitude of the signals. The signal analysis led to the following observations:

- The amplitudes of the test signals are different for different materials, independent of the type of damage. For our tests: 15 and 30 for CFRP versus 20 and 40 for Al.
- For the same material, the amplitudes of the signal are extremely different depending on the type of damage. For our tests, amplitudes for the case of non-penetration were precisely double those observed for penetration damage.
- The shape of the signals is different in 2 ways: non-penetration signals have a different shape than penetration signals, and signal shape is also different in time from one material to the other (less modulations for Al signals)
- The width of signal peaks or the duration of maximum amplitude is different as a function of the type of damage, non-perforation and perforation

These observation trends were independent of particle velocity or target thickness. In the first two tests, the CFRP targets had the same thicknesses but were tested at different velocities. In the second two tests, the Al targets had different thicknesses and were tested at different velocities. The observation trends revealed by the time frequency analysis should be validated by a larger number of future tests on different materials. Once this data is gathered, it will represent a basis for the creation of an automatic process that will recognize the damage in real-time for different materials that are used in space. In general terms, for the four tests the time frequency analysis provides clear characteristics, the most important being the frequency amplitude. This new knowledge represents a basis for future investigation and constitutes a starting point for development of a real-time MMOD health monitoring system.

Future Work

The main direction for future steps is closely related to the necessity to validate these results through further HVI testing, simulations with complementary time-frequency analysis of the signal and the development of a real-time method of detection and identification of damage. It is critical to perform further HVI tests, and as a first step we will use the same launcher in a more controlled environment. The results will lead to better observation of the moment of impact, eliminate the impacts of secondary fragments and the sabot, and improve velocity control and sabot separation.

Precise velocity control has an important role in controlling the type of damage. Improved sabot separation will eliminate this secondary impact on the target and provide a clean shot. The presence of multiple secondary impacts however, could be a positive effect since it more closely mimics the effects of impacts in a space environment and the response of materials and structures become closer to reality. Three series of HVI tests should be planned corresponding to three ranges of velocities; low, medium and high. In the near future low- velocity HVI tests should be conducted at an average speed of 1.5-1.7 km/s. In the more distant future the velocities should be increased; HVI tests at speeds up to 4.5 - 5 km/s (medium velocity range), followed by tests at speeds up to 8 km/s (high velocity range). These series of tests can be done using a new two-stage light gas gun at a Canadian facility in New Brunswick [9] or using the implosion gun at the same Shock Wave Laboratory, which allows tests at impact velocities up to 9 km/s [10]. Preparation of these tests and time frequency analysis of the data will involve a large amount of work over multiple years.

Closely related to the HVI tests is work in the area of time frequency signal analysis. Considerable resources are required to analyze recorded signals in order to apply a valid method that will lead to real-time identification of the types of damage on different types of materials.

Using time frequency signal analysis for HVI tests performed in low and high velocity regimes is complex and observation trends may be different than those presented here due to phase transformation of the material which occurs at such large impact speeds. Further time frequency analysis will enable continued development of the in-house TF-Analysis software [6-8], ideally suited for analysis and reduction of multi-sensor spectro-temporal steady and transient data. Methods incorporated into the TF-Analysis will be improved to more efficiently extract the primary features of the impact signals and make the results more user friendly and compatible with other time frequency software solutions. The results of time frequency analysis will open other directions of research including automation of damage detection. A software package based on the characteristics presented here could provide real-time information about the status of the target, which could be a space bumper or another element of a space structure. This research work will provide a new efficient tool for automation of damage detection based on a large collection of data on different categories of space materials.

ACKNOWLEDGMENT

This project has been made possible by precious support from the collaborative research and development grant of Natural Sciences and Engineering Research Council of Canada (NSERC)(No.8482) and the Fonds de recherche du Québec - Nature et technologies (FRQNT).

REFERENCES

1. R.A. Clegg, D.M. White, W. Riedel, W. Harwick "Hypervelocity impact damage prediction in composites: Part I—material model and characterisation" *International Journal of Impact Engineering* 33 (2006) 190–200
2. W. Riedel, H. Nahme, D.M. White, R.A. Clegg "Hypervelocity impact damage prediction in composites: Part II – experimental investigations and simulations" *International Journal of Impact Engineering* 33 (2006) 670–680
3. Anthony Devito "The combustion of bulk metals in a high-speed oxidizing flow", Masters thesis, McGill University Montreal, Quebec 2014-4-15
4. National instruments, <http://sine.ni.com/nips/cds/view/p/lang/fr/nid/202664>
5. PCB Piezotronics, <http://www.pcb.com/Products.aspx?m=352C33>
6. A. Oulmane, A.A. Lakis and N. Mureithi. 2013, A Method for Analyzing Rotating Machinery Faults using Time-Frequency Application. *International Journal of Condition Monitoring and Diagnostic Engineering Management* Volume 16 No2, April 2013 pages 21-34.
7. Oulmane, A., Lakis, A.A., Mureithi, N., and Safizadeh, M.S., June 2009, The Application of Time-Frequency Analysis in Rotating Machinery Fault Diagnosis, 22 nd International Congress and Exhibition on Condition Monitoring and Diagnostic Engineering Management, San Sebastian, Spain, pp 597-583.
8. Mahvash, A., Lakis A.A., 2014, "Independent Component Analysis as Applied to Vibration Source Separation and Fault Diagnosis", *Journal of vibration and control*, online: August 2014, DOI: 10.1177/107756314544349.
9. IADC WG3 "IADC Protection manual" IADC-04-03, Version 4.0, April 12, 2011
10. B. Aissa, K. Tagziria, W. Jamroz, E. Haddad, M. Asgar-Khan, S. V. Hoa , J. Loiseau, J. Verreault, A. Higgins "Monitoring with Fiber sensors and Self-Healing of CFRP Laminates Exposed to Hypervelocity Small Pellets Simulating Space Debris", 12th International Symposium on Materials in the Space Environment (IMSE-12) 24-28 September 2012.
11. A. Bettella, A. Francesconi, D. Pavarin, C. Giacomuzzo, F. Angrilli "Application of Wavelet Transform to analyze acceleration signals generated by HVI on thin aluminum plates and all-aluminum honeycomb sandwich panels" *International Journal of Impact Engineering* 35 (2008) 1427–1434
12. Karl F. Graff "Wave motion in elastic solids", Courier Corporation, 1975 – Science.
13. Lei Wang, F.G. Yuan "Group velocity and characteristic wave curves of Lamb waves in composites: Modeling and experiments" *Composites Science and Technology*, Volume 67, Issues 7-8, June 2007, Pages 1370–1384
14. H. Choi and W. J. Williams, "Improved time-frequency representation of multicomponent signals using exponential kernels," *IEEE. Trans. Acoustics, Speech, Signal Processing*, vol. 37, no. 6, pp. 862–871, June 1989.
15. Howard A. Gaberson, "Autocorrelation approaches to time frequency analysis of machinery vibration signals"
16. Howard A. Gaberson, "Application of Choi-Williams reduced Interference time frequency distribution to machinery diagnostics"
17. M. A. Hamstad, "Comparison of Wavelet transform and Choi-Williams distribution to determine group velocities for different acoustic emission sensors"
18. L. E. Iliescu, A. A. Lakis, A. Abou – Antoun "Hypervelocity Impact (HVI) Tests & Signal Recordings", *Universal Journal of Aeronautical & Aerospace Sciences* 2 (2014), 80-113
19. W. Goldsmith, "Impact. The theory of physical behavior of colliding solids" Courier Corporation, 2001-11-01 - 379 pages

20. William H. Prosser, Michael R. Gorman and Donald H. Humes, “Acoustic Emission Signals in Thin Plates Produced by Impact Damage”, *Journal of Acoustic Emission*, Vol. 17(1-2), (June, 1999), pp. 29-36.
21. William H. Prosser, Michael R. Gorman, John Dorigi “Extensional and Flexural Waves in a Thin-Walled Graphite/Epoxy Tube” *Journal of Composite Materials* Vol. 26(14), 1992, pp. 418-427
22. A. Oulmane, A.A.Lakis and N. Mureithi, Application of Fourier Descriptors & Artificial Neural Network to Bearing Vibration Signals for Fault Detection & Classification. *Universal Journal of Aeronautical & Aerospace Sciences* 2 (2014), 37-54.
23. Jean-Baptiste Vergniaud, Matthieu Guyot, Michel Lambert, Frank Schäfer, Shannon Ryan, Stefan Hiermaier, and Emma Taylor. Structural vibrations induced by HVI - Application to the Gaia spacecraft. *International journal of impact engineering* 35, No. 12, pp.1836-1843 (2008).
24. Francesconi, A., Pavarin, D., Bettella, A., Giacomuzzo, C., Faraud, M., Destefanis, R., Lambert, M., Angrilli, F. Generation of transient vibrations on aluminum honeycomb sandwich panels subjected to hypervelocity impacts, *International Journal of Impact Engineering* Volume 35, Issue 12, December 2008, Pages 1503–1509
25. F Schäfer, R Janovsky Impact sensor network for detection of hypervelocity impacts on spacecraft *Acta Astronautica* 61 (10), 901-911
26. Pavarin, D., Francesconi, A., Destefanis, R., Faraud, M., Lambert, M., Bettella, A., Giacomuzzo, C., Marucchi-Chierro, P.C., Ullio, R., Angrilli, F. Analysis of transient vibrations on complex targets representing elementary configurations of GOCE satellite (2008) *International Journal of Impact Engineering*, 35 (12), pp. 1709-1715.
27. Parzianello, G., Francesconi, A., Pavarin, D. An estimation method for the Shock Response Spectrum propagating into plates subjected to hypervelocity impact (2010) *Measurement: Journal of the International Measurement Confederation*, 43 (1), pp. 92-102
28. D. Pavarin, A. Francesconi, R. Destefanis, M. Lambert, A. Bettella, S. Debei, M. De Cecco, M. Faraud, C. Giacomuzzo, P.C. Marucchi-Chierro, G. Parzianello, B. Saggin, F. Angrilli, Acceleration fields induced by hypervelocity impacts on spacecraft structures, *International Journal of Impact Engineering* 33 (2006) 580-591.
29. H. Hertz, “On the contact of rigid elastic solids”, London (1896), p. 156.